SOLUTION OF TEAM BENCHMARK PROBLEM #10 (STEEL PLATES AROUND A COIL)

O. Biro
Graz University of Technology, Kopernikusgasse 24, A-8010 Graz, Austria

Abstract - **Problem No. 10 of the TEAM Workshops is solved by three different finite-element formulations using a magnetic vector potential with the Coulomb gauge and an electric scalar potential. Allowing the normal component of the vector potential to jump at iron/air interfaces yields results in good agreement with measurement data.**

Problem definition

This three-dimensional, non-linear, transient eddy current problem has been proposed by Prof. T. Nakata, N. Takahashi and K. Fujiwara as a benchmark problem for the TEAM Workshops. For convenience, its definition is repeated here [1].

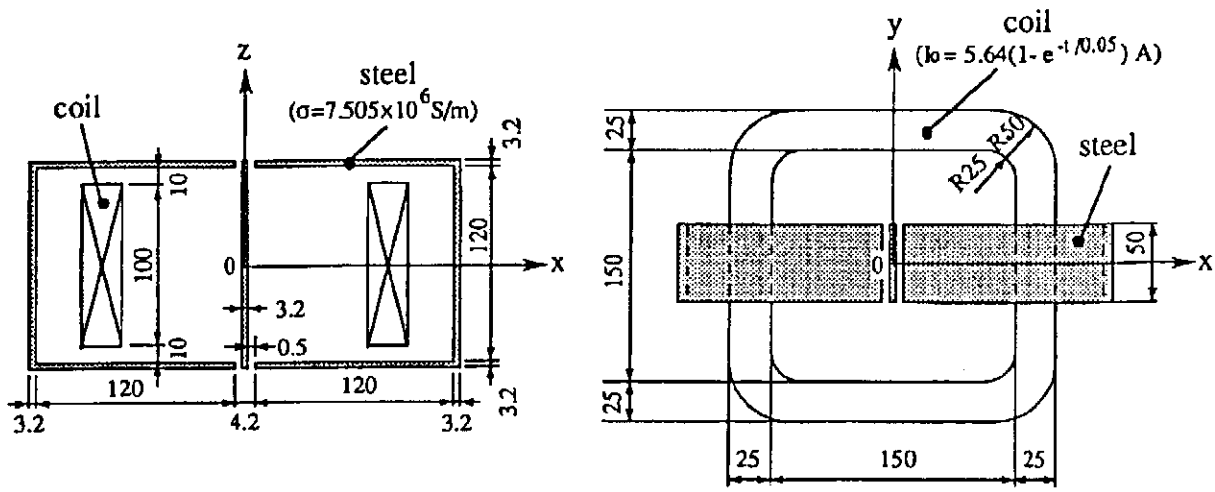

(a) front view (b) plan view

Fig. 1: Steel plates around a coil (dimensions in mm)

The model is shown in Fig. 1. An exciting coil is placed between two steel channels and a steel plate is inserted between the channels. The material of the steel is nonlinear, the magnetization curve is shown in Fig. 2. The curve can be approximated for high flux densities ($B > 1.8\ T$) as

$$\left.\begin{aligned} B &= \mu_0 H + (aH^2 + bH + c) \qquad (1.8T \le B \le 2.22T) \\ B &= \mu_0 H + M_S \qquad\qquad\qquad\quad (B \ge 2.22T) \end{aligned}\right\} \tag{1}$$

where μ_0 is the permeability of free space. The constants a, b and c are $-2.381\text{x}10^{-10}$, $2.327\text{x}10^{-5}$ and 1.590, respectively. M_S is the saturation magnetization (2.16 T) of the steel. The conductivity of the channels and of the center plate is $7.505\text{x}10^6$ S/m. The number of turns in the coil is 162. The exciting current varies with time as

$$I = \begin{cases} 0 & (t < 0) \\ I_m(1 - e^{-t/\tau}) & (t \geq 0) \end{cases} \tag{2}$$

The amplitude is I_m=5.64 A and the time constant is τ=0.05 s.

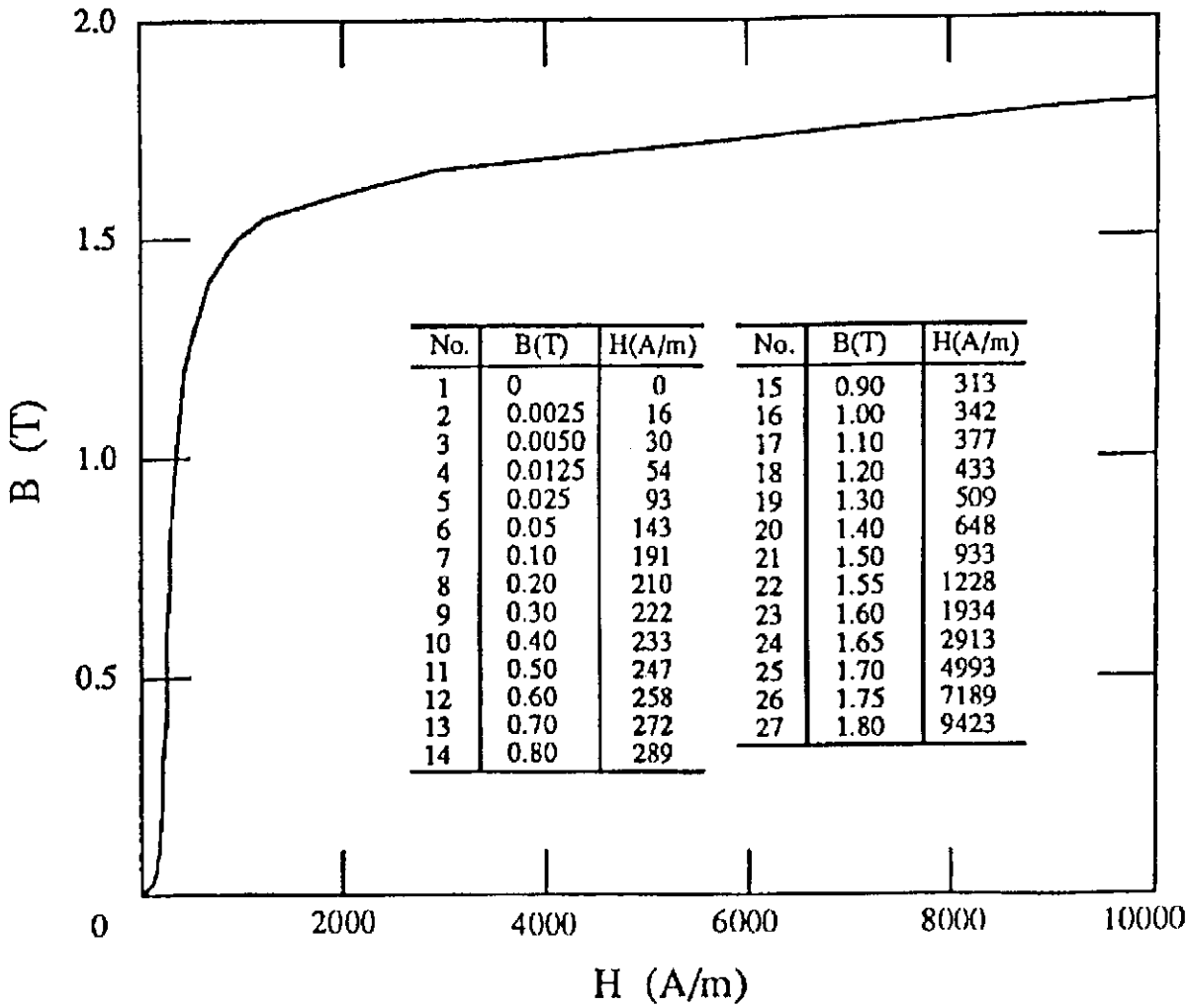

No.	B(T)	H(A/m)
1	0	0
2	0.0025	16
3	0.0050	30
4	0.0125	54
5	0.025	93
6	0.05	143
7	0.10	191
8	0.20	210
9	0.30	222
10	0.40	233
11	0.50	247
12	0.60	258
13	0.70	272
14	0.80	289

No.	B(T)	H(A/m)
15	0.90	313
16	1.00	342
17	1.10	377
18	1.20	433
19	1.30	509
20	1.40	648
21	1.50	933
22	1.55	1228
23	1.60	1934
24	1.65	2913
25	1.70	4993
26	1.75	7189
27	1.80	9423

Fig. 2: B-H curve of steel

It is required to find the time functions of the average flux density of the surfaces S_1, S_2 and S_3 shown in Fig. 3 and also the time functions of the current density at the points P_1, P_2 and P_3. These quantities have also been measured by the authors of [1].

The problem has been solved with the program package IGTEDDDY of the Institute for Fundamentals and Theory in Electrical Engineering of the Graz University of Technology. Three solutions have been obtained by formulations using a magnetic vector potential throughout and an additional electric scalar potential in the eddy current region.

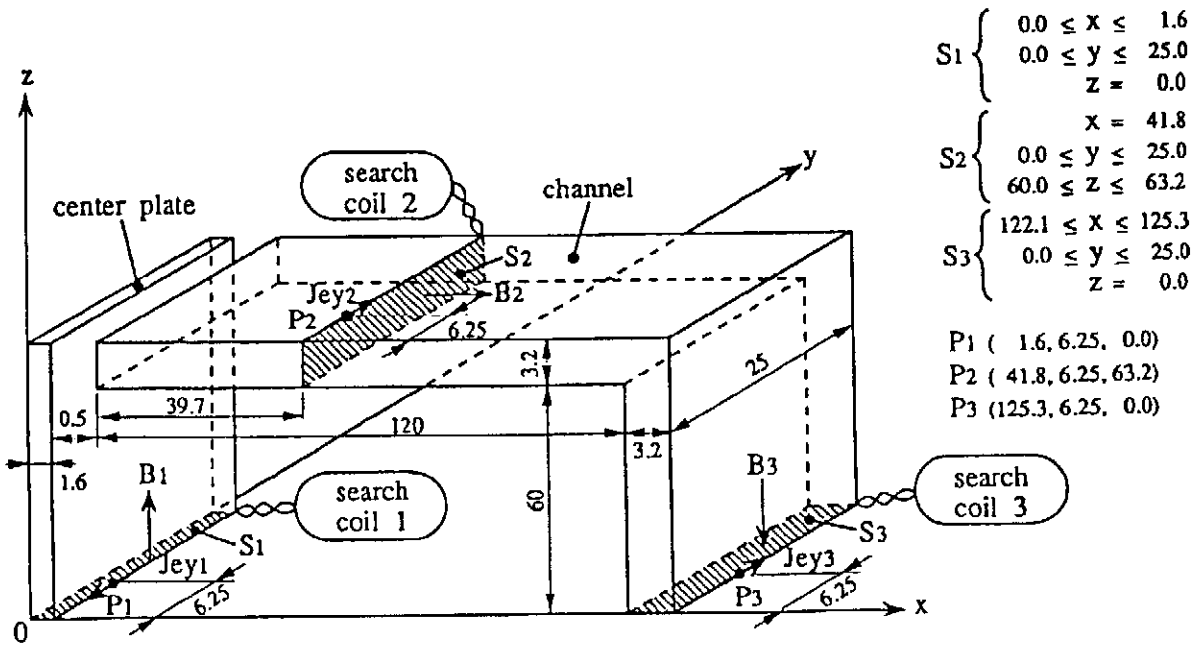

Fig. 3: Measurement positions for flux densities and current densities

A,V-A formulation, A_n continuous

This is the well-known **A**,V-**A** formulation [2] with the magnetic flux density and the electric field intensity derived from the potentials as

$$\mathbf{B} = \nabla \times \mathbf{A}, \tag{3}$$

$$\mathbf{E} = -\frac{\partial \mathbf{A}}{\partial t} - \nabla \frac{\partial v}{\partial t} \tag{4}$$

where **A** is the magnetic vector potential and v is the time integral of the electric scalar potential. The governing differential equations are

$$\nabla \times (\nu \nabla \times \mathbf{A}) - \nabla(\nu \nabla \cdot \mathbf{A}) + \sigma \frac{\partial \mathbf{A}}{\partial t} + \sigma \nabla \frac{\partial v}{\partial t} = \mathbf{0} \quad \text{in conductors,} \tag{5}$$

$$\nabla \cdot (-\sigma \frac{\partial \mathbf{A}}{\partial t} - \sigma \nabla \frac{\partial v}{\partial t}) = 0 \quad \text{in conductors,} \tag{6}$$

$$\nabla \times (\nu \nabla \times \mathbf{A}) - \nabla(\nu \nabla \cdot \mathbf{A}) = \mathbf{J} \quad \text{in non-conductors.} \tag{7}$$

These equations enforce the Coulomb gauge on the vector potential. Using nodal finite elements with one value for each component of **A** in each node, the vector potential is continuous.

The time functions of the average flux density and of the eddy current density in the positions required are plotted in Fig. 4 and in Fig. 5, respectively along with the measured results [1]. The numerical values are shown in Tables 1.1 and 1.2 whereas some further information on the computation is summarized in Table 1.3

Although the discretization is very fine, the average flux density is somewhat lower than measured while the current density is too high.

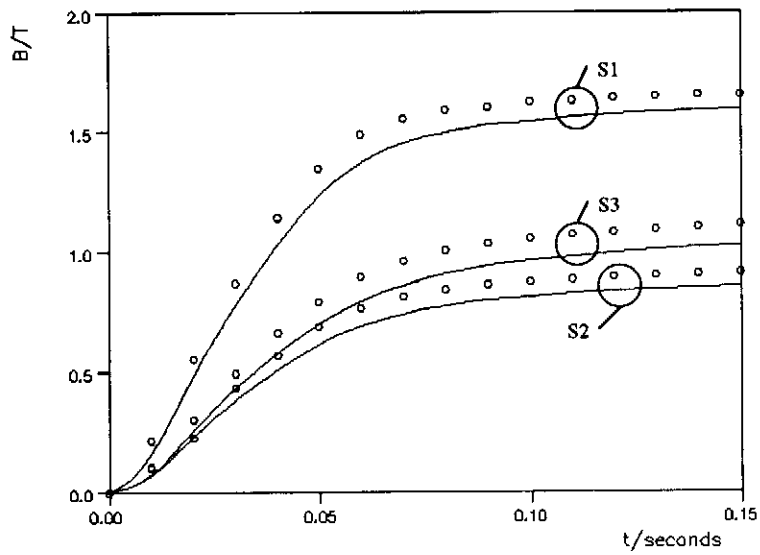

Fig. 4: Time functions of average flux densities, **A**,V-**A** formulation, A_n continuous
o o o o: measurement, ———: computation

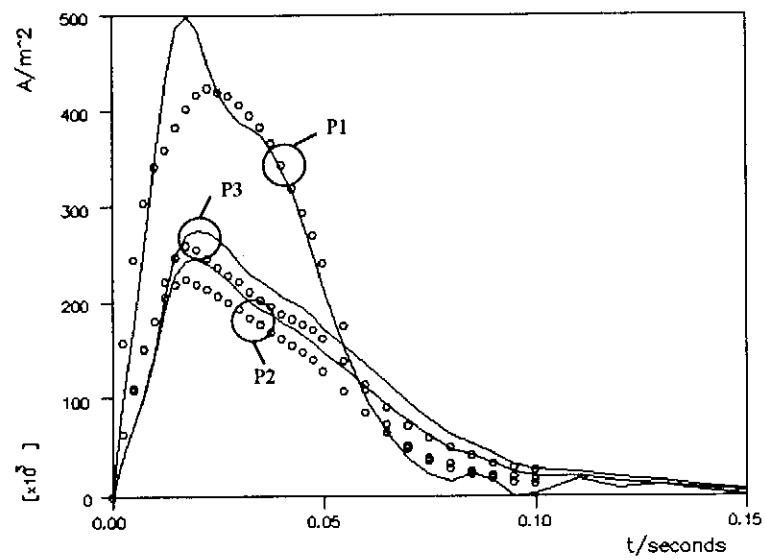

Fig. 5: Time functions of current densities, **A**,V-**A** formulation, A_n continuous
o o o o: measurement, ———: computation

time step	t(s)	position (coordinates in mm) S1 0.0<x< 1.6 0.0<y<25.0 z=0.0	S2 x=41.8 0.0<y<25.0 60.0<z<63.2	S3 122.1<x<125.3 0.0<y<25.0 z=0.0
1	0.0025	0.0211	0.0086	0.0090
2	0.0050	0.0548	0.0229	0.0238
3	0.0075	0.1016	0.0431	0.0447
4	0.0100	0.1631	0.0708	0.0741
5	0.0125	0.2375	0.1068	0.1141
6	0.0150	0.3203	0.1479	0.1607
7	0.0175	0.4056	0.1908	0.2098
8	0.0200	0.4894	0.2334	0.2590
9	0.0225	0.5694	0.2745	0.3068
10	0.0250	0.6448	0.3133	0.3521
11	0.0275	0.7163	0.3501	0.3948
12	0.0300	0.7846	0.3848	0.4350
13	0.0325	0.8503	0.4181	0.4733
14	0.0350	0.9139	0.4502	0.5101
15	0.0375	0.9752	0.4811	0.5457
16	0.0400	1.0338	0.5108	0.5798
17	0.0425	1.0896	0.5392	0.6126
18	0.0450	1.1421	0.5662	0.6440
19	0.0475	1.1908	0.5916	0.6737
20	0.0500	1.2356	0.6153	0.7018
21	0.0550	1.3114	0.6566	0.7518
22	0.0600	1.3722	0.6914	0.7951
23	0.0650	1.4191	0.7198	0.8316
24	0.0700	1.4541	0.7426	0.8618
25	0.0750	1.4791	0.7605	0.8866
26	0.0800	1.4970	0.7744	0.9069
27	0.0850	1.5147	0.7876	0.9248
28	0.0900	1.5279	0.7981	0.9398
29	0.0950	1.5339	0.8054	0.9514
30	0.1000	1.5397	0.8118	0.9615
31	0.1100	1.5598	0.8259	0.9807
32	0.1200	1.5713	0.8358	0.9952
33	0.0130	1.5834	0.8447	1.0077
34	0.0140	1.5899	0.8508	1.0168
35	0.0150	1.5928	0.8548	1.0234

Table 1.1: Average flux densities in steel (T)
A,V-**A** formulation, A_n continuous

time step	t(s)	position (coordinates in mm) P1 x=1.6 y=6.25 z=0.0	P2 x=41.8 y=6.25 z=63.2	P3 x=125.3 y=6.25 z=0.0
1	0.0025	1.0648	0.4366	0.4386
2	0.0050	1.7679	0.7297	0.7357
3	0.0075	2.5866	1.0506	1.0598
4	0.0100	3.5277	1.4662	1.5063
5	0.0125	4.3290	1.9602	2.0940
6	0.0150	4.8750	2.2969	2.5105
7	0.0175	4.9736	2.4331	2.7090
8	0.0200	4.8281	2.4520	2.7450
9	0.0225	4.4601	2.3954	2.7396
10	0.0250	4.1797	2.3063	2.6564
11	0.0275	3.9941	2.2157	2.5615
12	0.0300	3.8760	2.1009	2.3980
13	0.0325	3.8194	1.9982	2.2859
14	0.0350	3.7438	1.9240	2.2113
15	0.0375	3.5848	1.8598	2.1302
16	0.0400	3.3809	1.7875	2.0507
17	0.0425	3.1439	1.7260	2.0039
18	0.0450	2.8197	1.6526	1.9295
19	0.0475	2.4771	1.5668	1.8350
20	0.0500	2.1379	1.4761	1.7185
21	0.0550	1.5100	1.3081	1.5442
22	0.0600	0.9941	1.1196	1.3502
23	0.0650	0.6422	0.9297	1.1525
24	0.0700	0.3874	0.7620	0.9494
25	0.0750	0.2213	0.6091	0.7716
26	0.0800	0.1519	0.4821	0.6318
27	0.0850	0.2376	0.4290	0.5311
28	0.0900	0.1697	0.3426	0.4303
29	0.0950	-0.0041	0.2453	0.3208
30	0.1000	0.0295	0.2100	0.2670
31	0.1100	0.1796	0.2109	0.2507
32	0.1200	0.0873	0.1474	0.1882
33	0.0130	0.1158	0.1291	0.1597
34	0.0140	0.0493	0.0871	0.1086
35	0.0150	0.0128	0.0580	0.0737

Table 1.2: Y-component of eddy current densities on surface of steel (10^5 A/m^2)
A,V-**A** formulation, A_n continuous

No	Item	Specification
1	Code name	IGTEDDDY
2	Formulation	FEM (Finite Element Method)
3	Governing equations	$\nabla\times(\nu\nabla\times\mathbf{A})-\nabla(\nu\nabla\cdot\mathbf{A})+\sigma\frac{\partial\mathbf{A}}{\partial t}+\sigma\nabla\frac{\partial v}{\partial t}=\mathbf{0}$ in conductor $\nabla\times(\nu_0\nabla\times\mathbf{A})-\nabla(\nu_0\nabla\cdot\mathbf{A})=\mathbf{J}$ in vacuum
4	Solution variables	$\mathbf{A}$, v in conductor $\mathbf{A}$ in vacuum
5	Gauge condition	imposed on governing equations directly
6	Time difference method	θ method with θ=1 (backward difference)
7	Technique for non-linear problem	Incremental method
	Convergence criterion	mean ($\Delta\mu_r/\mu_r$) < 1% over all Gaussian points max ($\Delta\mu_r/\mu_r$) < 5% over all Gaussian points
8	Approximation method of B-H curve	straight lines
9	Technique for open boundary problem	truncation
10	Calculation method of magnetic field produced by exciting current	taking into account exciting current in governing equations directly
11	Property of coefficient matrix of linear equations	symmetric, sparse
12	Solution method for linear equations	ICCG
	Convergence criterion for iteration method	$\|Ax+b\|^2/\|b\|^2 < 10^{-10}$
13	Element type	hexahedron nodal element (20 nodes)
14	Number of elements	7,344
15	Number of nodes	32,986
16	Number of unknowns	88,079
17	Computer	name: DECstation 5000-200 speed: 24 MIPS main memory: 264 MB precision of data: 64 bits CPU time total: 443,117 s

Table 1.3: Computational data, **A**,V-**A** formulation, A_n continuous

A,V-A formulation, A_n discontinuous

The reason for the above behaviour is that once the Galerkin method is applied to the term $-\nabla(\nu\nabla\cdot\mathbf{A})$ in the differential equations (5) and (7), the continuity of the quantity $\nu\nabla\cdot\mathbf{A}$ becomes a natural interface condition [2]. Although $\nu\nabla\cdot\mathbf{A}$ is zero in the weak sense [2], it does in fact have a nonzero value due to the numerical approximation. This results in a tough constraint on $\nabla\cdot\mathbf{A}$ along interfaces where the reluctivity ν changes abruptly: there must be a jump in the divergence of the vector potential. Thus the accuracy is bound to be poor in the vicinity of such iron/air interfaces. In the present problem with thin ferromagnetic channels, the solution in the entire iron region is bound to be strongly influenced by this inaccuracy.

The problem can be overcome by refining the discretization, so that the condition $\nu\nabla\cdot\mathbf{A}=0$ is fulfilled with greater accuracy and the constraint on $\nabla\cdot\mathbf{A}$ has less effect. Indeed, the experience of the author has shown that a coarser mesh yields much poorer results than those shown above.

The constraint on the continuity of $\nu\nabla\cdot\mathbf{A}$ can be relaxed by allowing the normal component of the vector potential to be discontinuous on the iron/air interfaces [3]. As a consequence, the natural boundary condition $\nu\nabla\cdot\mathbf{A}=0$ results on the interface and the constraint on $\nabla\cdot\mathbf{A}$ is not present any more. At the application of finite element techniques, the normal component A_n is allowed to be discontinuous by employing four nodal variables in the nodes on

the interface: the two continuous tangential components and a normal component from the air region as well as one from the iron domain.

The time functions of the average flux density and of the eddy current density obtained by this method in the positions required are plotted in Fig. 6 and in Fig. 7, respectively with the measured results also shown. The numerical values are given in Tables 2.1 and 2.2 whereas some further information on the computation is summarized in Table 2.3

The agreement with the measured results is much better than for the case when A_n is continuous, although the same mesh has been used. The computation time is somewhat longer, due to the higher number of conjugate gradient iterations needed for the solution of the linear equations systems. It is expected that good results can be obtained by substantially coarser meshes, too.

$\mathbf{A_r}$,V-$\mathbf{A_r}$ formulation, $\mathbf{A_{rn}}$ discontinuous

The finite element mesh used in the above computations does not exactly fit the curved parts of the racetrack coil. This potentially leads to inaccuracies if the total vector potential defined by eq. (3) and the differential equations (5) to (7) are used since the representation of the current density may be inaccurate. To check whether this is the case, a reduced vector potential formulation has also been tried [3]. In this method the magnetic field $\mathbf{H}_S$ and vector potential $\mathbf{A}_S$ due to the coil in free space are split from the solution and it is therefore irrelevant whether the coil is exactly modelled by the finite element mesh.

The potentials are defined by

$$\mathbf{B} = \mu_0 \mathbf{H}_S + \nabla \times \mathbf{A}_r, \tag{8}$$

$$\mathbf{E} = -\frac{\partial \mathbf{A}_S}{\partial t} - \frac{\partial \mathbf{A}_r}{\partial t} - \nabla \frac{\partial v}{\partial t} \tag{9}$$

where $\mathbf{A}_r$ is the reduced vector potential. The governing differential equations are

$$\nabla \times (\nu \nabla \times \mathbf{A}_r) - \nabla(\nu \nabla \cdot \mathbf{A}_r) + \sigma \frac{\partial \mathbf{A}_r}{\partial t} + \sigma \nabla \frac{\partial v}{\partial t} = -\sigma \frac{\partial \mathbf{A}_S}{\partial t} - \nabla \times (\nu \mu_0 \mathbf{H}_S) \quad \text{in conductors,} \tag{10}$$

$$\nabla \cdot (-\sigma \frac{\partial \mathbf{A}_r}{\partial t} - \sigma \nabla \frac{\partial v}{\partial t}) = \nabla \cdot (\sigma \frac{\partial \mathbf{A}_S}{\partial t}) \quad \text{in conductors,} \tag{11}$$

$$\nabla \times (\nu_0 \nabla \times \mathbf{A}_r) - \nabla(\nu_0 \nabla \cdot \mathbf{A}_r) = \mathbf{0} \quad \text{in non-conductors.} \tag{12}$$

In order to avoid the inaccuracies due to the continuity of A_m in the vicinity of the iron/air interfaces, the normal component of the reduced vector potential has been allowed to be discontinuous here.

The time functions of the average flux density and of the eddy current density obtained by this method in the positions required are plotted in Fig. 8 and in Fig. 9, respectively with the measured results also shown. The numerical values are given in Tables 3.1 and 3.2 whereas some further information on the computation is summarized in Table 3.3.

The results are practically identical with those obtained by the total vector potential, i.e. the inaccurate modelling of the coils has caused no loss of precision in the **A**,V-**A** version.

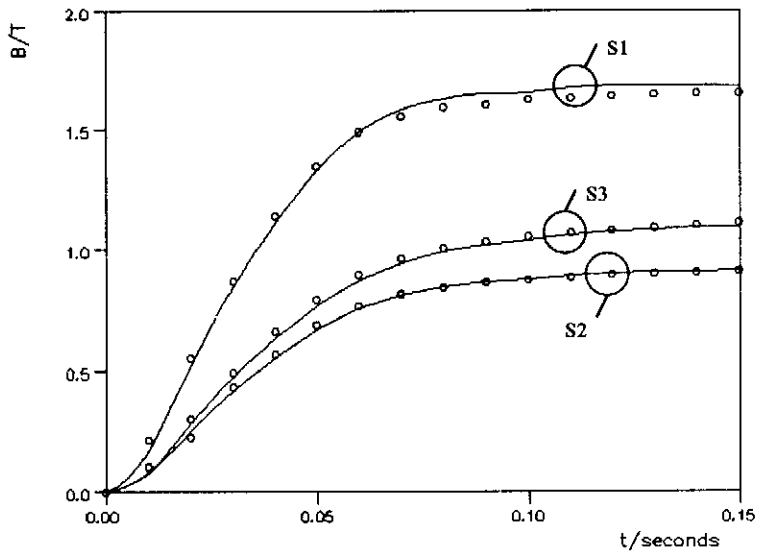

Fig. 6: Time functions of average flux densities, **A**,V-**A** formulation, A_n discontinuous
o o o o: measurement, ———: computation

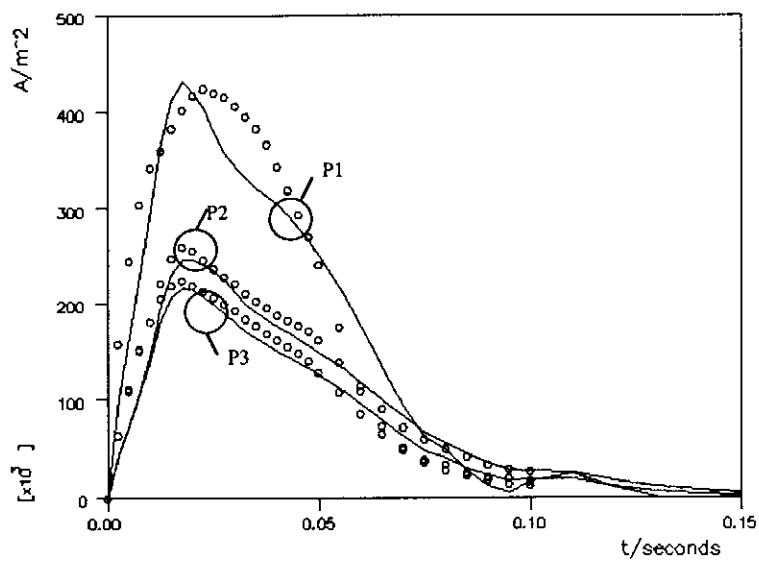

Fig. 7: Time functions of current densities, **A**,V-**A** formulation, A_n discontinuous
o o o o: measurement, ———: computation

time step	t(s)	position (coordinates in mm) S1 0.0<x< 1.6 0.0<y<25.0 z=0.0	S2 x=41.8 0.0<y<25.0 60.0<z<63.2	S3 122.1<x<125.3 0.0<y<25.0 z=0.0
1	0.0025	0.0222	0.0093	0.0098
2	0.0050	0.0582	0.0247	0.0259
3	0.0075	0.1090	0.0469	0.0491
4	0.0100	0.1753	0.0774	0.0818
5	0.0125	0.2564	0.1172	0.1266
6	0.0150	0.3465	0.1624	0.1783
7	0.0175	0.4394	0.2095	0.2325
8	0.0200	0.5300	0.2557	0.2861
9	0.0225	0.6170	0.3004	0.3381
10	0.0250	0.6991	0.3429	0.3878
11	0.0275	0.7765	0.3829	0.4345
12	0.0300	0.8501	0.4206	0.4783
13	0.0325	0.9204	0.4565	0.5198
14	0.0350	0.9879	0.4909	0.5595
15	0.0375	1.0528	0.5239	0.5976
16	0.0400	1.1153	0.5557	0.6343
17	0.0425	1.1751	0.5862	0.6696
18	0.0450	1.2319	0.6153	0.7034
19	0.0475	1.2854	0.6429	0.7356
20	0.0500	1.3355	0.6689	0.7662
21	0.0550	1.4217	0.7150	0.8212
22	0.0600	1.4918	0.7540	0.8687
23	0.0650	1.5457	0.7857	0.9088
24	0.0700	1.5842	0.8105	0.9416
25	0.0750	1.6094	0.8292	0.9677
26	0.0800	1.6298	0.8448	0.9896
27	0.0850	1.6412	0.8562	1.0069
28	0.0900	1.6465	0.8644	1.0203
29	0.0950	1.6488	0.8706	1.0310
30	0.1000	1.6565	0.8778	1.0417
31	0.1100	1.6768	0.8927	1.0620
32	0.1200	1.6858	0.9022	1.0763
33	0.0130	1.6872	0.9075	1.0856
34	0.0140	1.6852	0.9105	1.0916
35	0.0150	1.6826	0.9123	1.0955

Table 2.1: Average flux densities in steel (T)
A,V-**A** formulation, A_n discontinuous

time step	t(s)	position (coordinates in mm) P1 x=1.6 y=6.25 z=0.0	P2 x=41.8 y=6.25 z=63.2	P3 x=125.3 y=6.25 z=0.0
1	0.0025	1.0263	0.4403	0.4458
2	0.0050	1.6489	0.7311	0.7440
3	0.0075	2.2837	1.0457	1.0698
4	0.0100	2.9981	1.4119	1.4821
5	0.0125	3.6971	1.8179	1.9900
6	0.0150	4.1405	2.0703	2.3195
7	0.0175	4.3106	2.1641	2.4631
8	0.0200	4.2053	2.1471	2.4638
9	0.0225	4.0380	2.0731	2.4047
10	0.0250	3.7800	1.9908	2.3406
11	0.0275	3.5729	1.8946	2.2397
12	0.0300	3.4316	1.7901	2.1117
13	0.0325	3.3226	1.7002	1.9825
14	0.0350	3.2144	1.6262	1.9017
15	0.0375	3.1307	1.5610	1.8203
16	0.0400	3.0437	1.5029	1.7528
17	0.0425	2.9261	1.4455	1.6955
18	0.0450	2.7909	1.3803	1.6219
19	0.0475	2.6483	1.3144	1.5519
20	0.0500	2.5040	1.2477	1.4841
21	0.0550	2.1577	1.1114	1.3464
22	0.0600	1.7497	0.9513	1.1735
23	0.0650	1.3192	0.7846	0.9991
24	0.0700	0.9306	0.6234	0.8244
25	0.0750	0.6056	0.4805	0.6653
26	0.0800	0.4867	0.4056	0.5626
27	0.0850	0.2718	0.3037	0.4467
28	0.0900	0.1198	0.2248	0.3503
29	0.0950	0.0586	0.1741	0.2815
30	0.1000	0.1824	0.1934	0.2735
31	0.1100	0.2435	0.1931	0.2564
32	0.1200	0.1078	0.1252	0.1790
33	0.0130	0.0112	0.0738	0.1192
34	0.0140	-0.0316	0.0429	0.0774
35	0.0150	-0.0252	0.0275	0.0506

Table 2.2: Y-component of eddy current densities on surface of steel (10^5 A/m^2)
A,V-**A** formulation, A_n discontinuous

No	Item	Specification
1	Code name	IGTEDDDY
2	Formulation	FEM (Finite Element Method)
3	Governing equations	$\nabla\times(\nu\nabla\times\mathbf{A})-\nabla(\nu\nabla\cdot\mathbf{A})+\sigma\frac{\partial\mathbf{A}}{\partial t}+\sigma\nabla\frac{\partial v}{\partial t}=\mathbf{0}$ in conductor $\nabla\times(\nu_0\nabla\times\mathbf{A})-\nabla(\nu_0\nabla\cdot\mathbf{A})=\mathbf{J}$ in vacuum
4	Solution variables	$\mathbf{A}, \nu$ in conductor $\mathbf{A}$ in vacuum
5	Gauge condition	imposed on governing equations directly, A_n discontinuous on iron/air interface
6	Time difference method	θ method with θ=1 (backward difference)
7	Technique for non-linear problem	Incremental method
	Convergence criterion	mean ($\Delta\mu_r/\mu_r$) < 1% over all Gaussian points max ($\Delta\mu_r/\mu_r$) < 5% over all Gaussian points
8	Approximation method of B-H curve	straight lines
9	Technique for open boundary problem	truncation
10	Calculation method of magnetic field produced by exciting current	taking into account exciting current in governing equations directly
11	Property of coefficient matrix of linear equations	symmetric, sparse
12	Solution method for linear equations	ICCG
	Convergence criterion for iteration method	$\|Ax+b\|^2/\|b\|^2 < 10^{-10}$
13	Element type	hexahedron nodal element (20 nodes)
14	Number of elements	7,344
15	Number of nodes	32,986
16	Number of unknowns	89,278
17	Computer	name: DECstation 5000-200 speed: 24 MIPS main memory: 264 MB precision of data: 64 bits CPU time total: 663,663 s

Table 2.3: Computational data, **A**,V-**A** formulation, A_n discontinuous

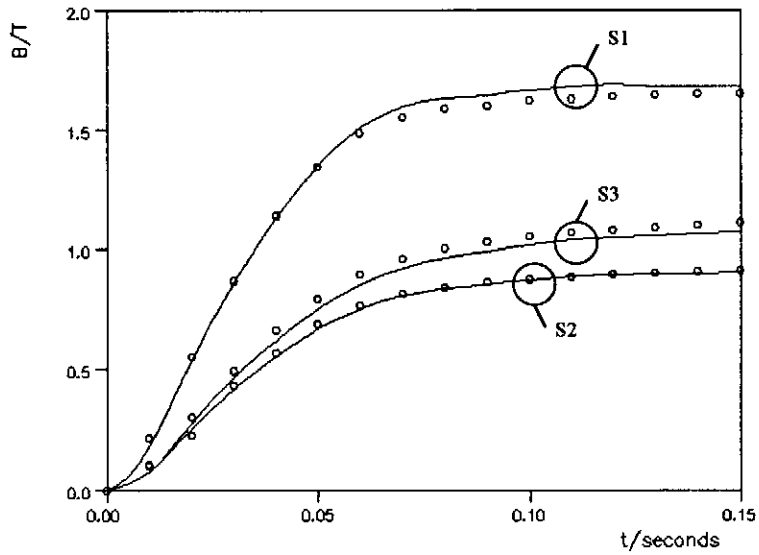

Fig. 8: Time functions of average flux densities, $\mathbf{A}_r$,V-$\mathbf{A}_r$ formulation, A_m discontinuous
o o o o: measurement, ———: computation

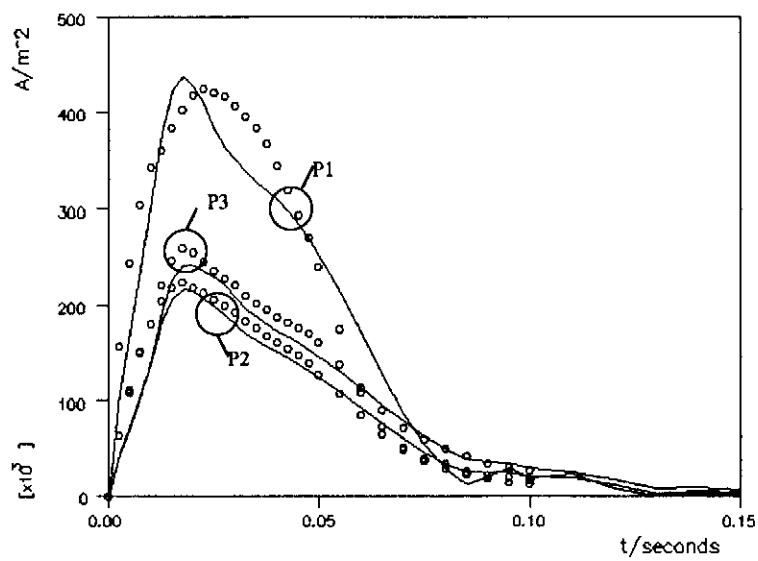

Fig. 9: Time functions of current densities, $\mathbf{A}_r$,V-$\mathbf{A}_r$ formulation, A_m discontinuous
o o o o: measurement, ———: computation

time step	t(s)	position (coordinates in mm) S1 0.0<x< 1.6 0.0<y<25.0 z=0.0	S2 x=41.8 0.0<y<25.0 60.0<z<63.2	S3 122.1<x<125.3 0.0<y<25.0 z=0.0
1	0.0025	0.0234	0.0093	0.0092
2	0.0050	0.0612	0.0249	0.0246
3	0.0075	0.1142	0.0474	0.0470
4	0.0100	0.1824	0.0781	0.0787
5	0.0125	0.2651	0.1179	0.1223
6	0.0150	0.3566	0.1632	0.1731
7	0.0175	0.4508	0.2103	0.2265
8	0.0200	0.5425	0.2565	0.2793
9	0.0225	0.6305	0.3011	0.3304
10	0.0250	0.7134	0.3435	0.3794
11	0.0275	0.7917	0.3836	0.4255
12	0.0300	0.8664	0.4214	0.4688
13	0.0325	0.9377	0.4574	0.5098
14	0.0350	1.0062	0.4918	0.5489
15	0.0375	1.0721	0.5249	0.5865
16	0.0400	1.1354	0.5567	0.6227
17	0.0425	1.1960	0.5872	0.6576
18	0.0450	1.2533	0.6163	0.6909
19	0.0475	1.3071	0.6438	0.7225
20	0.0500	1.3571	0.6696	0.7525
21	0.0550	1.4425	0.7150	0.8061
22	0.0600	1.5110	0.7530	0.8522
23	0.0650	1.5625	0.7835	0.8906
24	0.0700	1.5982	0.8070	0.9216
25	0.0750	1.6200	0.8242	0.9459
26	0.0800	1.6311	0.8364	0.9646
27	0.0850	1.6367	0.8453	0.9794
28	0.0900	1.6453	0.8542	0.9929
29	0.0950	1.6574	0.8636	1.0061
30	0.1000	1.6653	0.8711	1.0171
31	0.1100	1.6842	0.8854	1.0370
32	0.1200	1.6916	0.8942	1.0508
33	0.0130	1.6812	0.8952	1.0568
34	0.0140	1.6826	0.8993	1.0640
35	0.0150	1.6829	0.9024	1.0698

Table 3.1: Average flux densities in steel (T)
$\mathbf{A}_r$,V-$\mathbf{A}_r$ formulation, A_m discontinuous

time step	t(s)	position (coordinates in mm) P1 x=1.6 y=6.25 z=0.0	P2 x=41.8 y=6.25 z=63.2	P3 x=125.3 y=6.25 z=0.0
1	0.0025	1.0805	0.4390	0.4155
2	0.0050	1.7310	0.7360	0.7099
3	0.0075	2.3863	1.0575	1.0303
4	0.0100	3.0836	1.4188	1.4316
5	0.0125	3.7678	1.8206	1.9378
6	0.0150	4.2121	2.0724	2.2730
7	0.0175	4.3720	2.1633	2.4171
8	0.0200	4.2573	2.1450	2.4245
9	0.0225	4.0869	2.0678	2.3598
10	0.0250	3.8132	1.9864	2.3002
11	0.0275	3.6167	1.8924	2.2074
12	0.0300	3.4921	1.7916	2.0755
13	0.0325	3.3717	1.7007	1.9641
14	0.0350	3.2707	1.6273	1.8719
15	0.0375	3.1866	1.5630	1.8011
16	0.0400	3.0944	1.5038	1.7303
17	0.0425	2.9617	1.4444	1.6672
18	0.0450	2.8246	1.3779	1.5989
19	0.0475	2.6758	1.3089	1.5261
20	0.0500	2.5130	1.2350	1.4533
21	0.0550	2.1364	1.0942	1.3093
22	0.0600	1.6995	0.9275	1.1349
23	0.0650	1.2626	0.7554	0.9568
24	0.0700	0.8532	0.5922	0.7829
25	0.0750	0.5265	0.4450	0.6216
26	0.0800	0.2665	0.3246	0.4855
27	0.0850	0.1252	0.2455	0.3863
28	0.0900	0.2064	0.2399	0.3515
29	0.0950	0.2913	0.2474	0.3375
30	0.1000	0.1912	0.1981	0.2834
31	0.1100	0.2247	0.1855	0.2504
32	0.1200	0.0862	0.1171	0.1758
33	0.0130	-0.1320	0.0236	0.0809
34	0.0140	0.0220	0.0546	0.0907
35	0.0150	0.0108	0.0423	0.0730

Table 3.2: Y-component of eddy current densities on surface of steel (10^5 A/m^2)
$\mathbf{A}_r$,V-$\mathbf{A}_r$ formulation, A_m discontinuous

No	Item	Specification
1	Code name	IGTEDDDY
2	Formulation	FEM (Finite Element Method)
3	Governing equations	$\nabla\times(\nu\nabla\times\mathbf{A}_r)-\nabla(\nu\nabla\cdot\mathbf{A}_r)+\sigma\frac{\partial\mathbf{A}_r}{\partial t}+\sigma\nabla\frac{\partial\nu}{\partial t}=$ $-\sigma\frac{\partial\mathbf{A}_s}{\partial t}-\nabla\times(\nu\mu_0\mathbf{H}_s)$ in conductor $\nabla\times(\nu_0\nabla\times\mathbf{A}_r)-\nabla(\nu_0\nabla\cdot\mathbf{A}_r)=\mathbf{0}$ in vacuum
4	Solution variables	$\mathbf{A}_r$, ν in conductor $\mathbf{A}_r$ in vacuum
5	Gauge condition	imposed on governing equations directly, A_m discontinuous on iron/air interface
6	Time difference method	θ method with θ=1 (backward difference)
7	Technique for non-linear problem	Incremental method
	Convergence criterion	mean ($\Delta\mu_r/\mu_r$) < 1% over all Gaussian points max ($\Delta\mu_r/\mu_r$) < 5% over all Gaussian points
8	Approximation method of B-H curve	straight lines
9	Technique for open boundary problem	truncation
10	Calculation method of magnetic field produced by exciting current	Biot-Savart law (analytical) Biot-Savart law (numerical)
11	Property of coefficient matrix of linear equations	symmetric, sparse
12	Solution method for linear equations	ICCG
	Convergence criterion for iteration method	$\|Ax+b\|^2/\|b\|^2 < 10^{-10}$
13	Element type	hexahedron nodal element (20 nodes)
14	Number of elements	7,344
15	Number of nodes	32,986
16	Number of unknowns	89,278
17	Computer	name: DECstation 5000-200 speed: 24 MIPS main memory: 264 MB precision of data: 64 bits CPU time total: 685,377 s

Table 3.3: Computational data, $\mathbf{A}_r$,V-$\mathbf{A}_r$ formulation, A_m discontinuous

References

[1] T. Nakata, N. Takahashi and K. Fujiwara, "Summary of results for benchmark problem 10 (steel plates around a coil)", in R. Albanese, E. Coccorese, Y. Crutzen and P. Molfino (ed.), *Proc., Third International TEAM Workshop,* Sorrento, Italy, 12-13 July 1991, pp. 211-221

[2] O. Biro, K. Preis, "On the use of the magnetic vector potential in the finite element analysis of 3-D eddy currents", IEEE Transactions on Magnetics, vol. MAG-25, 1989, pp. 3145-3159

[3] K. Preis, I. Bardi, O. Biro, C. Magele, W. Renhart, K.R. Richter and G. Vrisk, "Numerical analysis of 3-D magnetostatic fields", IEEE Transactions on Magnetics, vol. MAG-27, 1991, pp. 3798-3803